# Dynamics of the chain of forced oscillators with long-range interaction: From synchronization to chaos

G. M. Zaslavsky
*Courant Institute of Mathematical Sciences, New York University, 251 Mercer St., New York, New York 10012, USA and Department of Physics, New York University, 2-4 Washington Place, New York, New York 10003, USA*

M. Edelman
*Courant Institute of Mathematical Sciences, New York University, 251 Mercer St., New York, New York 10012, USA*

V. E. Tarasov
*Courant Institute of Mathematical Sciences, New York University, 251 Mercer St., New York, New York 10012, USA and Skobeltsyn Institute of Nuclear Physics, Moscow State University, Moscow 119992, Russia*

(Received 25 July 2007; accepted 7 November 2007; published online 12 December 2007)

We consider a chain of nonlinear oscillators with long-range interaction of the type $1/l^{1+\alpha}$, where $l$ is a distance between oscillators and $0<\alpha<2$. In the continuous limit, the system's dynamics is described by a fractional generalization of the Ginzburg-Landau equation with complex coefficients. Such a system has a new parameter $\alpha$ that is responsible for the complexity of the medium and that strongly influences possible regimes of the dynamics, especially near $\alpha=2$ and $\alpha=1$. We study different spatiotemporal patterns of the dynamics depending on $\alpha$ and show transitions from synchronization of the motion to broad-spectrum oscillations and to chaos. © *2007 American Institute of Physics*. [DOI: 10.1063/1.2819537]

**A chain of nonlinear interacting oscillators is a model of the widespread investigation of different physical phenomena such as synchronized behavior of the system, bifurcations to different regimes, spatiotemporal turbulent or chaotic dynamics, different instabilities, appearance of defects, and many others. The long-range interaction between oscillators leads to a new qualitative dynamics and thermodynamics. Our consideration is related to the power-law long-range interaction that makes it possible to find new regimes and to establish a link of the corresponding equations of motion to the equations with fractional derivatives.**

## I. INTRODUCTION

The goal of the paper is to consider different dynamical regimes, from synchronization to chaos and turbulence, in a chain of large number of coupled nonlinear oscillators with long-range interaction (LRI) of a power type. The potential of interaction is nonlocal and proportional to $1/l^{1+\alpha}$ with $l$ as a distance between oscillators and $0<\alpha<2$ $(\alpha\neq 1)$. It will be called $\alpha$-interaction. Transitions between different regimes of the chain behavior are considered as a function of $\alpha$. In the continuous limit the system reduces to the fractional generalization of the Ginzburg-Landau (FGL) equation and the chain of oscillators can be considered as a discretized model of FGL, called DFGL. The considered model has complex coefficients and it can also be related to a fractional generalization of the complex nonlinear Schrödinger equation. Let us comment that the main physical feature of the model is the LRI of a power type, and the analogy to the equation with fractional derivative plays an auxiliary role.

The literature related to this type of problem is fairly waste and we would refer only to some reviews and closely related articles. The complex Ginzburg-Landau equation is considered, typically, for pattern formation in different media.[1–3] CGL equation appears in numerous physical models (see, for example, Refs. 4–7). Long-range interaction with finite radius of interaction was considered for complex media in Refs. 8 and 9 and for the $\alpha$-interaction in Refs. 10–14. Different regimes of synchronization in the chain of coupled oscillators with nearest neighbor interaction can be found in reviews[15,16] while the synchronization with $\alpha$-interaction for DFGL was obtained in Refs. 17 and 18. The FGL equation was introduced in Ref. 19 to describe the wave propagation in complex media, when the dispersion law has fractional power of the wave number. The related case appears in description of weak turbulence.[20] More examples related to the chains with LRI and their solution of the soliton or breather type can be found in Refs. 21 and 22.

The main part of this paper is a numerical simulation of the chain of $N=512$ coupled oscillators with $\alpha$-interaction and constant external force that pump energy into the system. This system links to the FGL equation in a continuous limit based on the formal procedure introduced in Refs. 17 and 23.

It will be shown that the forcing oscillatory media with LRI exhibits transition to chaos and turbulence when $\alpha$ decreases. As another interesting regime, we found a "collectivized" limit cycle that has a broad spectrum in phase space

 

+of any individual oscillator. Such a cycle exists within an interval of $\alpha$.

In Sec. II, we present the basic equation for coupled oscillators and their continuous media limit. This part includes some modified version of the results of Refs. 17 and 24. In Sec. III, we consider fractional generalization of the CGL equation and some of its stability criteria. Sections IV–VI play an auxiliary role in identifying an interesting domain of parameters to be studied. The main numerical results are presented in Secs. VII–IX. It is important to note that the main studied object is the chain of nonlinear oscillators, and a part of the obtained results, can be appropriate for the complex FGL equation at least for a finite time. The FGL equation can also be used for some estimates of the critical parameters to change the regimes of behavior of the chain of oscillators.

## II. CHAIN OF OSCILLATORS WITH LONG-RANGE INTERACTION

Following Ref. 24, let us introduce the system by the equations

$$\frac{dZ_n}{dt} + g_0 \sum_{\substack{m=-\infty \\ m\neq n}}^{+\infty} J_\alpha(|n-m|)[Z_m(t) - Z_n(t)] + F(Z_n(t)) = 0, \quad (1)$$

where $F(Z) = \partial V(Z)/\partial Z$, $g_0$ as an interaction constant, and interparticle interaction is

$$J_\alpha(|n-m|) = \frac{1}{|n-m|^{\alpha+1}}, \quad (\alpha > 0), \quad (2)$$

and the usual linear oscillator term $Z_n(t)$ can be included into $V[Z_n(t)]$.

A continuous limit of Eq. (1) can be defined by a transform operation from $Z_n(t)$ to $Z(x,t)$.[17,23] First, define $Z_n(t)$ as Fourier coefficients of some function $\hat{Z}(k,t)$, $k \in [-K_0/2, K_0/2]$, i.e.,

$$\hat{Z}(t,k) = \sum_{n=-\infty}^{+\infty} Z_n(t) e^{-ikx_n} = \mathcal{F}_\Delta\{Z_n(t)\}, \quad (3)$$

where $x_n = n\Delta x$, and $\Delta x = 2\pi/K_0$ is a distance between nearest particles in the chain, and

$$Z_n(t) = \frac{1}{K_0} \int_{-K_0/2}^{+K_0/2} dk \hat{Z}(t,k) e^{ikx_n} = \mathcal{F}_\Delta^{-1}[\hat{Z}(t,k)]. \quad (4)$$

Second, in the limit $\Delta x \to 0$ $(K_0 \to \infty)$ replace $Z_n(t) = (2\pi/K_0) Z(x_n,t) \to Z(x,t)dx$, and $x_n = n\Delta x = 2\pi n/K_0 \to x$. In this limit, Eqs. (3) and (4) are transformed into the integrals

$$\tilde{Z}(t,k) = \int_{-\infty}^{+\infty} dx e^{-ikx} Z(t,x) = \mathcal{F}[Z(t,x)] = \lim_{\Delta x \to 0} \mathcal{F}_\Delta[Z_n(t)], \quad (5)$$

$$Z(t,x) = \frac{1}{2\pi} \int_{-\infty}^{+\infty} dk e^{ikx} \tilde{Z}(t,k) = \mathcal{F}^{-1}[\tilde{Z}(t,k)] = \lim_{\Delta x \to 0} \mathcal{F}_\Delta^{-1}[\hat{Z}(t,k)]. \quad (6)$$

Applying Eq. (3) to Eq. (1) and performing the limit Eq. (5), we obtain

$$\frac{\partial Z(t,x)}{\partial t} + g_\alpha \frac{\partial^\alpha Z(t,x)}{\partial |x|^\alpha} + F(Z(t,x)) = 0 \quad (1 < \alpha < 2), \quad (7)$$

where $\partial^\alpha/\partial|x|^\alpha$ is the fractional Riesz derivative[25] defined by

$$\frac{\partial^\alpha Z(t,x)}{\partial |x|^\alpha} = \mathcal{F}^{-1}\{|k|^\alpha \tilde{Z}(t,k)\}$$

and

$$g_\alpha = 2g_0 (\Delta x)^\alpha \Gamma(-\alpha) \cos\left(\frac{\pi\alpha}{2}\right) \quad (8)$$

is the renormalized interaction constant. Equations of type (7) with different nonlinear terms were considered in Refs. 17 and 23. For other values of $\alpha$ one can obtain a similar equation to Eq. (7) by performing the corresponding transform operation.

## III. COMPLEX NONSTATIONARY GINZBURG-LANDAU EQUATION

Consider a chain of the nearest-neighbor coupled nonlinear oscillators described by the equations

$$\frac{d}{dt} Z_n(t) = (1+ia) Z_n - (1+ib)|Z_n|^2 Z_n + (c_1 + ic_2)(Z_{n+1} - 2Z_n + Z_{n-1}), \quad (9)$$

where we assume that all oscillators have the same internal parameters. Such equations can be obtained from Eq. (1) for $\alpha = \infty$ and the corresponding choice of $g_0$ and $V(Z_n)$. Transition to the continuous medium assumes that the difference $Z_{n+1} - Z_n$ is of the same order as $\Delta x$, and the interaction constants $c_1$ and $c_2$ are fairly large. Setting $c_1 = g(\Delta x)^{-2}$, $c_2 = gc(\Delta x)^{-2}$ with new constants $g$ and $c$, we get

$$\frac{\partial}{\partial t} Z = (1+ia) Z - (1+ib)|Z|^2 Z + g(1+ic) \frac{\partial^2}{\partial x^2} Z, \quad (10)$$

which is a time-dependent complex Ginzburg-Landau (CGL) equation.

Let us come back to the equation for nonlinear oscillators with fractional long-range coupling

$$\frac{d}{dt} Z_n = (1+ia) Z_n - (1+ib)|Z_n|^2 Z_n + g_0 \sum_{m\neq n} \frac{1}{|n-m|^{\alpha+1}} (Z_n - Z_m), \quad (11)$$

where $Z_n = Z_n(t)$ is the position of the $n$th oscillator in the complex plane, $1 < \alpha < 2$, and the corresponding choice of

$F(Z_n)=(1+i\alpha)Z_n-(1+ib)|Z_n^2|Z_n$ has been done. The corresponding equation in the continuous limit is

$$\frac{\partial}{\partial t}Z=(1+ia)Z-(1+ib)|Z|^2Z+g(1+ic)\frac{\partial^\alpha}{\partial|x|^\alpha}Z \quad (1<\alpha<2,\ \alpha\neq 1), \tag{12}$$

where $g(1+ic)=g_0a_\alpha$,

$$a_\alpha=2\Gamma(-\alpha)\cos(\pi\alpha/2). \tag{13}$$

Equation (12) is a fractional generalization of the complex nonstationary Ginzburg-Landau (FGL) equation (10). Equation (11) is the same as Eq. (1) with a special choice of $V$. It was suggested in Ref. 19 to describe complex media with fractional dispersion law.

The FGL equation (12) can be presented as the system of real equations

$$\begin{aligned}\frac{d}{dt}X&=\left(1-g\frac{\partial^\alpha}{\partial|x|^\alpha}\right)X-\left(a-gc\frac{\partial^\alpha}{\partial|x|^\alpha}\right)Y\\&\quad-(X^2+Y^2)(X-bY),\\\frac{d}{dt}Y&=\left(1-g\frac{\partial^\alpha}{\partial|x|^\alpha}\right)Y+\left(a-gc\frac{\partial^\alpha}{\partial|x|^\alpha}\right)X\\&\quad-(X^2+Y^2)(Y+bX),\end{aligned} \tag{14}$$

where $X=X(t,x)$ and $Y=Y(t,x)$ are real and imaginary parts of $Z(t,x)$.

The results of numerical simulation of the system (11) can be applied for a finite time for the FGL equation (12) although it is well known that typically the discrete systems are more chaotic than their continuous counterpart. Discretized equations can be presented in a form of the map. Return back to the continuous differential equations from the map leads to a new term that is equivalent to a high frequency perturbation. This term can generate an area of chaotic dynamics in phase space, even if it does not exist without this additional term, or the term can increase already existing chaos.[32] The system (11) will be called discretized FGL equation or simply DFGL.

## IV. PARAMETERS OF STABILITY OF PLANE-WAVE SOLUTION

In this section, we obtain some conditions of instability that will be implemented in numerical simulations of the system (11). These conditions are easy to derive and interpret considering the FGL equation.

To obtain a particular solution of the FGL equation (12) with a fixed wave number $K$, we consider $Z$ in the form

$$Z(x,t)=A(K,t)e^{iKx}. \tag{15}$$

Substitution of Eq. (15) into Eq. (12) gives

$$\frac{\partial}{\partial t}A(K,t)=(1+ia)A-(1+ib)|A|^2A-g(1+ic)|K|^\alpha A. \tag{16}$$

The plane-wave solution of Eq. (16) is

$$A(x,t)=(1-g|K|^\alpha)^{1/2}e^{iKx-i\omega_\alpha(K)t},\quad 1-g|K|^\alpha>0, \tag{17}$$

where

$$\omega_\alpha(K)=(b-a)+(c-b)g|K|^\alpha,\quad 1-g|K|^\alpha>0. \tag{18}$$

The solution of Eq. (17) can be presented as

$$\begin{aligned}X_0(x,t)&=(1-g|K|^\alpha)^{1/2}\cos(Kx-\omega_\alpha(K)t+\theta_0),\\Y_0(x,t)&=(1-g|K|^\alpha)^{1/2}\sin(Kx-\omega_\alpha(K)t+\theta_0),\\&\quad 1-g|K|^\alpha>0,\end{aligned} \tag{19}$$

where $X=X(x,t)=\mathrm{Re}\,Z(x,t)$, $Y=Y(x,t)=\mathrm{Im}\,Z(x,t)$, and $\theta_0$ is an arbitrary constant phase. These solutions can be interpreted as a synchronized state of the oscillatory medium. In fact, it will be shown by simulation that the synchronized solution exists also for the DFGL equation (11).

To obtain the stability condition, consider the variation of Eq. (16) near solution (19),

$$\frac{d}{dt}\delta X=A_{11}\delta X+A_{12}\delta Y,\quad \frac{d}{dt}\delta Y=A_{21}\delta X+A_{22}\delta Y, \tag{20}$$

where $\delta X$ and $\delta Y$ are small variations of $X$ and $Y$, and

$$\begin{aligned}A_{11}&=1-g|K|^\alpha-2X_0(X_0-bY_0)-(X_0^2+Y_0^2),\\A_{12}&=-a+gc|K|^\alpha-2Y_0(X_0-bY_0)+b(X_0^2+Y_0^2),\\A_{21}&=a-gc|K|^\alpha-2X_0(Y_0+bX_0)-b(X_0^2+Y_0^2),\\A_{22}&=1-g|K|^\alpha-2Y_0(Y_0+bX_0)-(X_0^2+Y_0^2).\end{aligned} \tag{21}$$

The conditions of asymptotic stability for Eq. (20) are

$$A_{11}+A_{22}<0,\quad A_{11}A_{22}-A_{12}A_{21}<0. \tag{22}$$

Substitution of Eqs. (19) and (21) into Eq. (22) gives

$$A_{11}+A_{22}=-2(1-g|K|^\alpha), \tag{23}$$

$$A_{11}A_{22}-A_{12}A_{21}=[b(1-g|K|^\alpha)-(a-gc|K|^\alpha)]\times[3b(1-g|K|^\alpha)-(a-gc|K|^\alpha)]. \tag{24}$$

Then the conditions (22) have the form

$$\begin{aligned}&1-g|K|^\alpha>0,\\&1-g|K|^\alpha<a/b-(c/b)g|K|^\alpha<3(1-g|K|^\alpha),\end{aligned} \tag{25}$$

i.e., the plane-wave solution (17) is unstable if the parameters $a$, $b$, $c$, and $g$ do not satisfy Eq. (25). Condition (25) defines the region of parameters for plane waves where the synchronization can exist.

In the numerical simulation, we use the parameters

$$a=-1.2,\quad b=-2,\quad c=2,\quad g=1. \tag{26}$$

Then Eq. (25) gives the inequalities

$$0<1-|K|^\alpha<0.6+|K|^\alpha<3(1-|K|^\alpha). \tag{27}$$

As a result, the plane-wave solution with $E=0$ is stable for

$$0.2 < |K|^{\alpha} < 0.6, \quad (1 < \alpha < 2). \tag{28}$$

In our numerical simulation, we use the initial conditions with

$$|K| = 2\pi/64 \approx 0.09817 \tag{29}$$

that is, $K$ is in the unstable region for $1<\alpha<2$. In the following the initial conditions with perturbation $E \neq 0$ will be out of the boundaries (28), and evolution of the initially unstable states will be studied.

## V. MAPPING THE NUMERICAL DATA

Numerical results are obtained as solutions of the coupled equations

$$\frac{d}{dt}Z_n = (1+ia)Z_n - (1+ib)|Z_n|^2 Z_n + \frac{1+ic}{a_\alpha(\Delta x)^\alpha}\sum_{m\neq n}^{N}\frac{1}{|n-m|^{\alpha+1}}(Z_n - Z_m) + E, \tag{30}$$

where $n=1,\ldots,N$, $\Delta x=1$, and $E$ is a constant external force. In simulations, the number of oscillators was $N=512$, and the external force was $E=0.3$. In the continuous limit, Eq. (30) transforms into the FGL equation with forcing.

For all sets of parameters, we integrate the DFGL equations with the initial conditions

$$Z_n(0) = A_0 e^{iKn}, \tag{31}$$

where $|K|=2\pi/T$, the space period is $T=64$, and $A_0$ is an initial amplitude. Numerical solutions were stored at each $t_q=0.005q$, where $q \in \mathbb{N}$.

To visualize the numerical solution we consider the following values:

(1) We plot the surface $|Z(x,t)|^2$ and the phase-space projection of the central oscillator $(n=0, x_n=0)$ formed by the variables,

$$A(t) = |Z(0,t)|^2, \quad \dot{A}(t) = \frac{dA(t)}{dt}. \tag{32}$$

(2) In addition to Eq. (32), we plot $Y(t)=\mathrm{Im}[Z(0,t)]$ versus $X(t)=\mathrm{Re}[Z(0,t)]$ for better resolution of the central oscillator behavior.

(3) We calculate the discrete Fourier transform of the sequence $Z(0,t_q)$ defined as

$$\hat{Z}_n(\omega_j) = \frac{1}{Q}\sum_{q=0}^{Q-1} Z_n(t_q)\exp(-i\omega_j t_q), \tag{33}$$

$$Z_n(t_q) = \sum_{j=0}^{Q-1} \hat{Z}_n(\omega_j)\exp(i\omega_j t_n), \tag{34}$$

where $\omega_j=2\pi j/Q$, $(j=0,\ldots,Q-1)$. The spectrum of the sequence $Z_n(t_q)$ for $q=0,\ldots,Q-1$ is given by

$$S_j \equiv S(\omega_j) = |\hat{Z}_n(\omega_j)|^2. \tag{35}$$

Our main goal is to compare solutions of the DFGL equation for different values of $\alpha \in (1,2)$ and consider emergence of chaotic dynamics of the chain of oscillators as a function of $\alpha$. The larger $\alpha$, the weaker the long-range interaction.

In the simulations, we consider the following plots:

(a) Color plots present surfaces $|Z_n(t)|^2$ versus $t$ and $n$;

(b) Plane $(A, dA/dt)$ displays a projection of the trajectory of the central oscillator [see definition in Eq. (32)];

(c) Plane $(\mathrm{Re}\,Z, \mathrm{Im}\,Z)$ displays a projection of the complex amplitude $Z=Z(0,t)$ of the central oscillator as a function of time;

(d) Plots $(\log_{10}\omega, \log_{10} S)$ describe the spectrum of time oscillations of $Z(0,t)$ [see definition in Eq. (35)].

## VI. SOME NUMERICAL RESULTS FOR THE CGL EQUATION

In this section, we provide some numerical results derived in Refs. 17 and 26–29 for the complex Ginzburg-Landau (CGL) equation in order to compare them, obtained for $\alpha=2$, with our results for $\alpha<2$. For many other results and details, see Refs. 1, 3, and 15.

(a) In Ref. 27, the CGL equation has been considered for the parameters

$$\alpha = 2, \quad a = 0 \quad b = 1.333, \quad c = -1, \tag{36}$$

and the phase turbulence has been observed.

(b) It was shown in Ref. 28 that for the parameters

$$\alpha = 2, \quad a = 0, \quad b = -1.4, \quad c = 0.6, \tag{37}$$

solution of the CGL equation has chaotic states and it is spatiotemporal intermittent.

(c) It was found in Ref. 28 that for the parameters

$$\alpha = 2, \quad a = 0, \quad b = 1.2, \quad c = -0.6, \tag{38}$$

solution of the CGL equation has zig-zagging holes near the transition to the plane waves.

(d) In Ref. 26 the CGL equation was considered for the parameters

$$\alpha = 2, \quad a = -1.2, \quad b = -2, \quad c = 2. \tag{39}$$

For $E=0.35$ the solution displays pitchforks without defects while for $E=0.23$ the rare defects were observed.

(e) In Ref. 17, the FGL equation was considered for the parameters

$$1 < \alpha < 2, \quad a = 1, \quad b = 0, \quad c = 70. \tag{40}$$

It was shown that the solution had one stable fixed point for $\alpha_0<\alpha<2$, $(\alpha_0=1.51)$ that corresponds to synchronization of oscillators. Decreasing $\alpha$ below $\alpha_0$ leads to a limit cycle via the Hopf bifurcation.

## VII. TRANSITION FROM SYNCHRONIZATION TO TURBULENCE

Regular propagation in time of the initial state of the chain of oscillators will be called synchronization. To consider $\alpha$-dependence of transition from synchronization to turbulence near $\alpha=2$, we use the parameters

$$a = -1.2, \quad b = -2, \quad c = 2, \quad A_0 = 0.2, \tag{41}$$

similar to Eq. (39) that were used in Ref. 26 for the CGL equation (12), but for the chain of oscillators with $\alpha \neq 2$. The

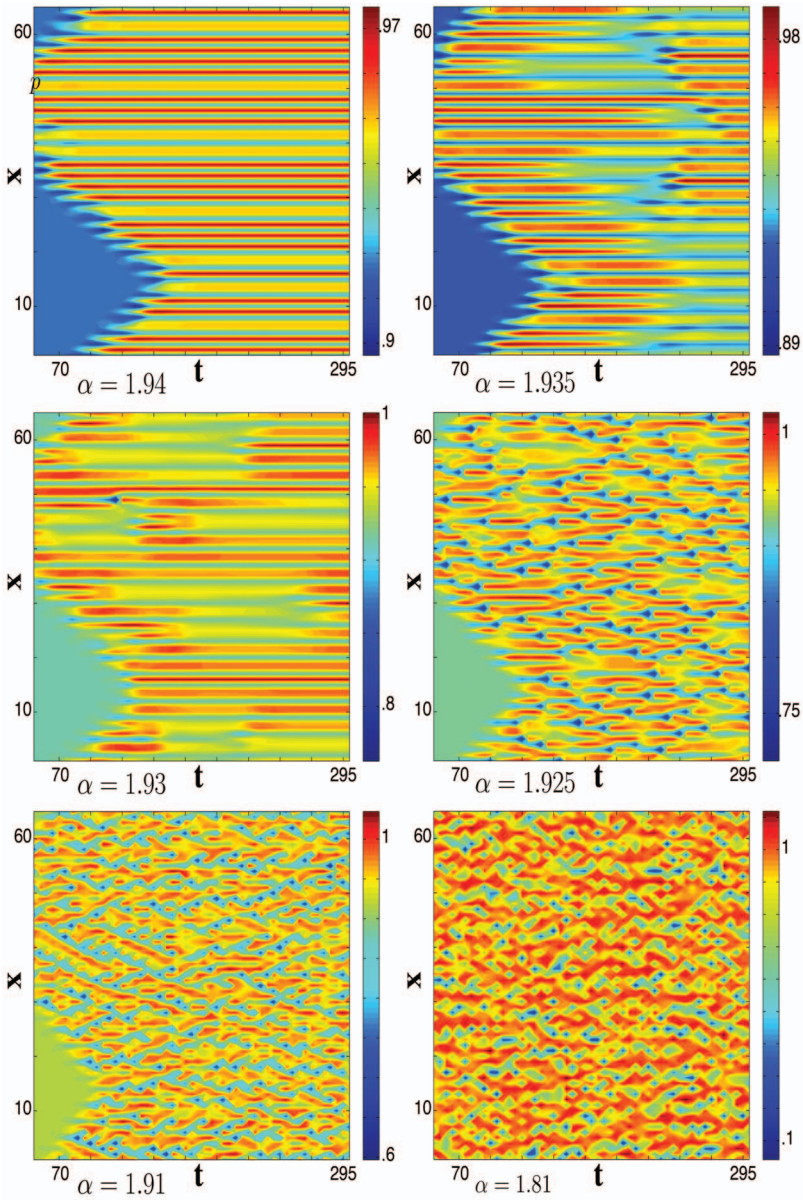


FIG. 1. (Color) Alpha-dependence of transition from synchronization to turbulence near $\alpha=2$. Surfaces of $|Z_n(t)|^2$ vs $t$ and $x=n$ for $\alpha=1.940$, $\alpha=1.935$, $\alpha=1.930$, $\alpha=1.925$, $\alpha=1.910$, $\alpha=1.810$. Simulations are realized for FGL equation with parameters $a=-1.2$, $b=-2$, $c=2$, $A_0=0.2$.

simulation was performed for the chain of 512 oscillators with parameters equivalent to Eq. (41).

In Fig. 1, the surfaces of $|Z_n(t)|^2$ versus $t$ and $x=n$ for $\alpha=1.940$, $\alpha=1.935$, $\alpha=1.930$, $\alpha=1.925$, $\alpha=1.910$, $\alpha=1.810$ are shown. For $\alpha=1.940$, we have a regular space structure of the plane-wave-type. For $\alpha=1.935$, there is a space modulation, which deforms the regular space structure. For $\alpha=1.930$, we can see the appearance of defects and pitchforks. For $\alpha=1.925$, the structure in the space-time demonstrates sharp and drastic changes. There exist many defects and pitchforks. For $\alpha=1.910$, the number of defects and pitchforks is increased, and some pitchforks are joined. For $\alpha=1.810$, we can see chaos and turbulence, and synchronization is completely lost. We see that the amplitude turbulence is characterized by persistent creation and annihilation of pitchforks. The decreasing order of the fractional derivative means increasing the role of the LRI. It is worthwhile to comment that the loss of synchronization and the emergence of amplitude turbulence is fairly sharp with a fairly small change of $\alpha$.

In Fig. 2 the plane $(\mathrm{Re}\, Z, \mathrm{Im}\, Z)$ shows projection of the complex amplitude $Z=Z(0,t)$ of the central oscillator as a function of time for $\alpha=1.940$, $\alpha=1.930$, $\alpha=1.925$, $\alpha=1.810$. For $\alpha=1.94$ and $\alpha=1.93$, there is a stable node, which means the existence of synchronization. The dynamics of the chain appears to be sensitive to the changes of $\alpha$ even in the second decimal digit. Conformation of that can also be found in Fig. 3, where the plane $(A, dA/dt)$ shows projection of the trajectory of the central oscillator and $A(t)=|Z(0,t)|^2$. For $\alpha=1.94$ and $\alpha=1.93$, the attracting point that corresponds to synchronization of the chain of oscillators is clearly seen. Characteristics of the turbulent motion, shown in Fig. 1. for $\alpha=1.925$, $\alpha=1.91$, $\alpha=1.81$, are different from the cases of larger $\alpha$. This difference can be better recognized from Figs. 2–4. Particularly, in Fig. 2. for $\alpha-1.925$ and

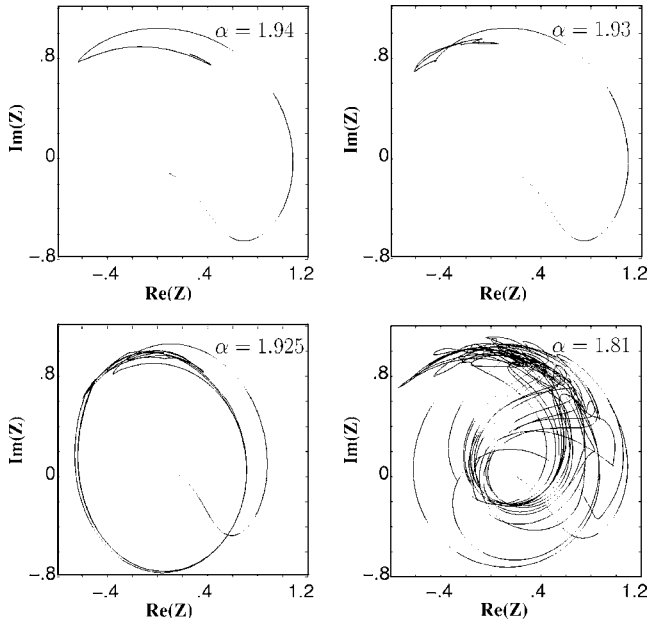


FIG. 2. Alpha-dependence of transition from synchronization to turbulence near $\alpha=2$. Plane $(\mathrm{Re}\,Z,\mathrm{Im}\,Z)$ shows projection of the complex amplitude $Z=Z(0,t)$ of the central oscillator as a function of time for $\alpha=1.940$, $\alpha=1.930$, $\alpha=1.925$, $\alpha=1.810$.

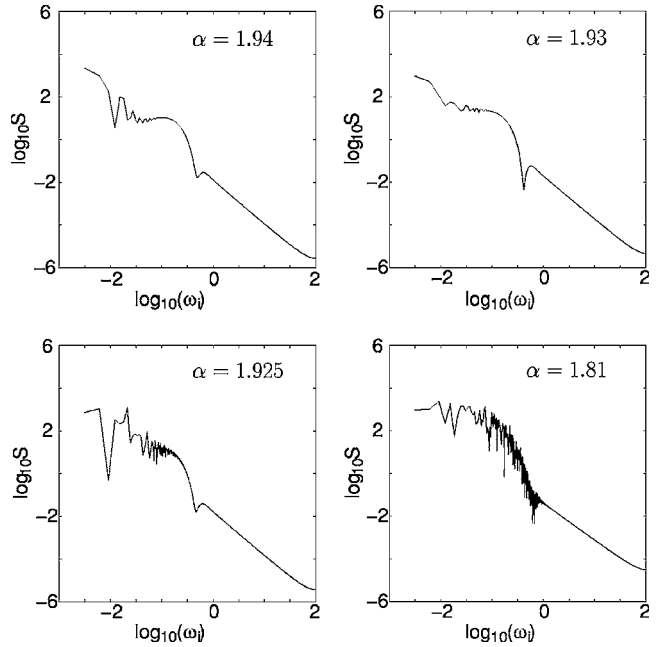


FIG. 4. Alpha-dependence of transition from synchronization to turbulence near $\alpha=2$. Spectrum of time oscillations of $Z(0,t)$ [see definition in Eq. (35)] for $\alpha=1.940$, $\alpha=1.930$, $\alpha=1.925$, $\alpha=1.810$.

$\alpha=1.81$ behavior of $\mathrm{Re}\,Z=\mathrm{Re}\,Z(0,t)$ and $\mathrm{Im}\,Z=\mathrm{Im}\,Z(0,t)$ displays a disordered process that on the plane $(A,dA/dt)$ in Fig. 3. reveals a structure similar to what is usually observed for chaotic attractors. Nevertheless, a more specific statement needs more detailed analysis since our system is open and has many degrees of freedom. While the plane $(A,dA/dt)$ displays a similarity to the chaotic attractor for one oscillator, more precise formulation and definitions are necessary. From this point the definition of a turbulent regime does not have

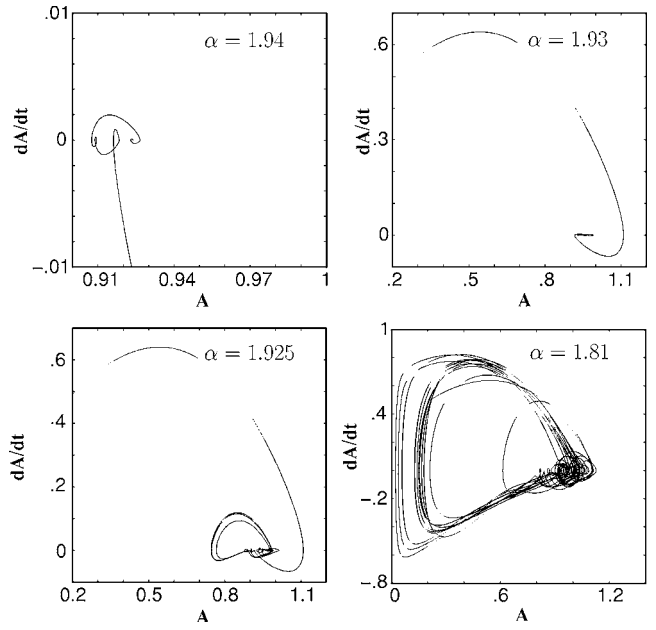


FIG. 3. Alpha-dependence of transition from synchronization to turbulence near $\alpha=2$. Plane $(A,dA/dt)$ shows projection of the trajectory of the central oscillator in phase space, where $A(t)=|Z(0,t)|^2$ for $\alpha=1.940$, $\alpha=1.930$, $\alpha=1.925$, $\alpha=1.810$.

at the moment exact dynamical background and we use this notion just to claim a space-time disordered motion. One more comment is related to the comparison of the plots for $\alpha=1.94$ and $\alpha=1.93$. While there is no visually significant difference for the central oscillator in Figs. 2 and 3, the difference is essential for the collective motion as it seems from Fig. 1. Similarly, we demonstrate the difference between $\alpha=1.925$ and $\alpha=1.81$.

In Fig. 4 we show the spectrum of time oscillations of $Z(0,t)$ [see definition in Eq. (35)] for $\alpha=1.940$, $\alpha=1.930$, $\alpha=1.925$, $\alpha=1.810$. For $\alpha=1.94$ and $\alpha=1.93$, the spectrum has small numbers of harmonics, and it corresponds to the regime of synchronization in the oscillator medium. For $\alpha=1.925$, the spectrum is filled by additional harmonics. For $\alpha=1.81$, the spectrum has a dense set of frequencies for the region $0.1<\omega<1$ that reflects the chaos behavior and turbulence of the oscillator medium. For the region $1<\omega<100$, we can see the integer power-law for the spectrum $S(\omega)\sim\omega^{-2}$ that corresponds to the main frequency dependence of Eq. (16).

## VIII. TRAVELING WAVES AND BROADENING OF THE LIMIT CYCLE

A large number of oscillators and periodic boundary conditions permit us to consider localized traveling waves (see, for example, for discrete systems in Refs. 30 and 31). Such waves were observed in our system (30) near the values of $\alpha\lesssim 2$ and disappear near $\alpha\approx 1$. In the latter case, space-temporary localized topological defects will also be demonstrated.

The simulation was performed for the parameters

$$a=1,\quad b=0,\quad c=2,\quad A_0=0.2. \tag{42}$$

For the value $b=0$, the nonlinear term is real.

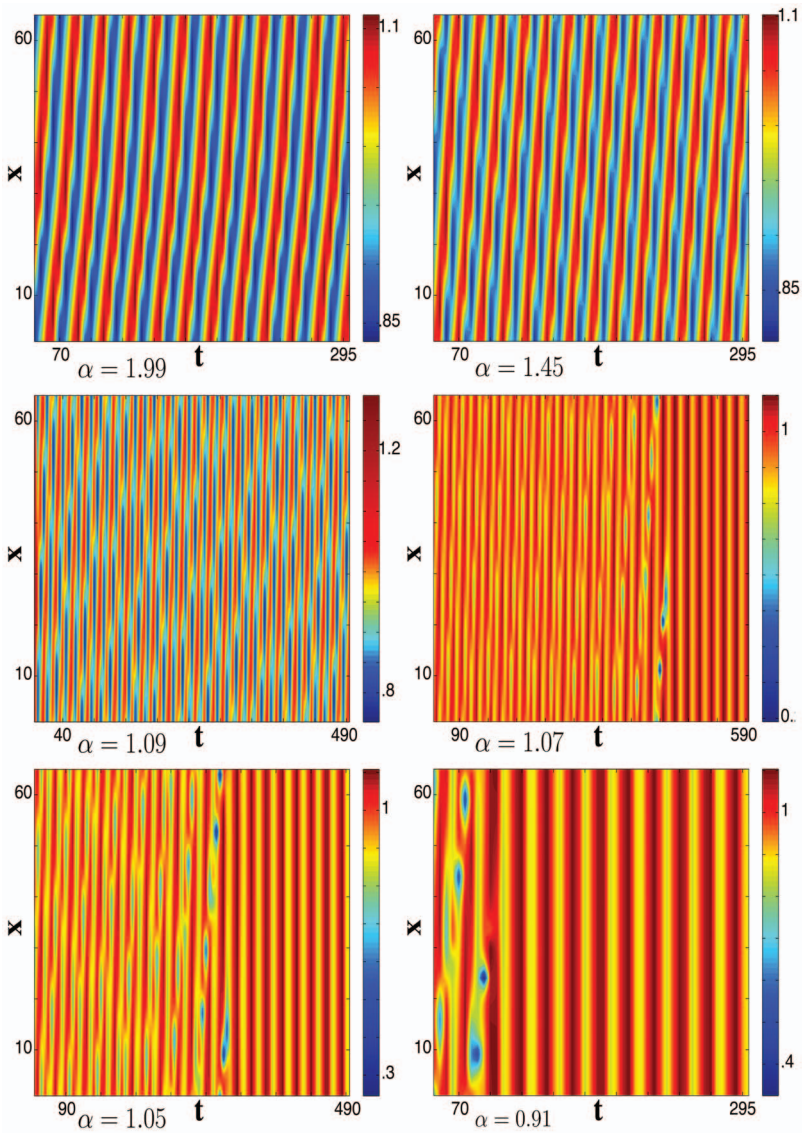


FIG. 5. (Color) Broadening of limit cycle. Wave front deinclination. Surfaces of $|Z_n(t)|^2$ vs $t$ and $x=n$ for $\alpha=1.99$, $\alpha=1.45$, $\alpha=1.09$, $\alpha=1.07$, $\alpha=1.05$, $\alpha=0.91$. Simulations are realized for the FGL equation with parameters $a=1$, $b=0$, $c=2$, $A_0=0.2$.

The waves propagation can be characterized by the group velocity $v_{\alpha,g}=\partial\omega_\alpha(K)/\partial K$. From Eq. (18), we obtain

$$v_{\alpha,g}=\alpha(c-b)g|K|^{\alpha-1}. \tag{43}$$

The phase velocity is

$$v_{\alpha,\mathrm{ph}}=\omega_\alpha(K)/K=\frac{b-a}{K}+(c-b)g|K|^{\alpha-1}. \tag{44}$$

For the parameters used in the simulations we have $|v_{\alpha,g}|>|v_{\alpha,g}|$. In our simulation $K=2\pi/64$. For our simulation $K=2\pi/64$, and the decrease of the order $\alpha$ leads to the increase of the group and phase velocities.

The corresponding simulation is shown in Figs. 5–8 for the surfaces $|Z_n(t)|^2$ (Fig. 5), Re $Z$ and Im $Z$ plane (Fig. 6), $(dA/dt,A)$-plane (Fig. 7) and spectrum $S(\omega)$ in Fig. 8. Each of the plates has the some additional information about solutions. There is a strong difference between values $\alpha=1.99$, $\alpha=1.45$, and $\alpha=1.07$, $\alpha=1.05$, $\alpha=0.91$ while the case of $\alpha=1.09$ is not clear since the finite time of simulation ($t<1000$). The first case ($\alpha=1.99$, $\alpha=1.45$) shows traveling waves along $x$ with regular (periodic or quasiperiodic) patterns. In Figs. 5 and 6, we observe the approach of the solution to a limit cycle with a few harmonics in the spectrum (Fig. 8). At the same time the smaller the $\alpha$, the smaller scales (larger values of $K$) enter the solution.

For $\alpha$ close to one ($\alpha=1.07$, $\alpha=1.05$, $\alpha=0.91$) a fairly irregular pattern of traveling wave declines at some time, and synchronized oscillations take place. In the phase diagrams in Figs. 6 and 7 a broadened limit cycle type picture corresponds to collective oscillations of the chain with fairly rich spectrum presented in Fig. 8. The closer $\alpha$ is to one, the shorter the time break of traveling waves, and the synchronized breather-type solution appears. Since the growth of wave numbers $K$ of the solution, its amplitude can reach zero giving rise the topological defects.[3] Their appearance is clearly seen from Figs. 6 and 7 for $\alpha=1.05$ (see also Fig. 5), when the amplitude $A(t)=|Z(0,t)|^2$ reaches zero value. It is seen that for $\alpha=1.07$ and $\alpha=0.91$ the dynamics is close to the appearance of the topological defect. Zero of the complex field $Z$ result in singularity of the phase $\theta=\arg Z$. In two dimensions, points of singularities correspond to quantized vortices with topological charge

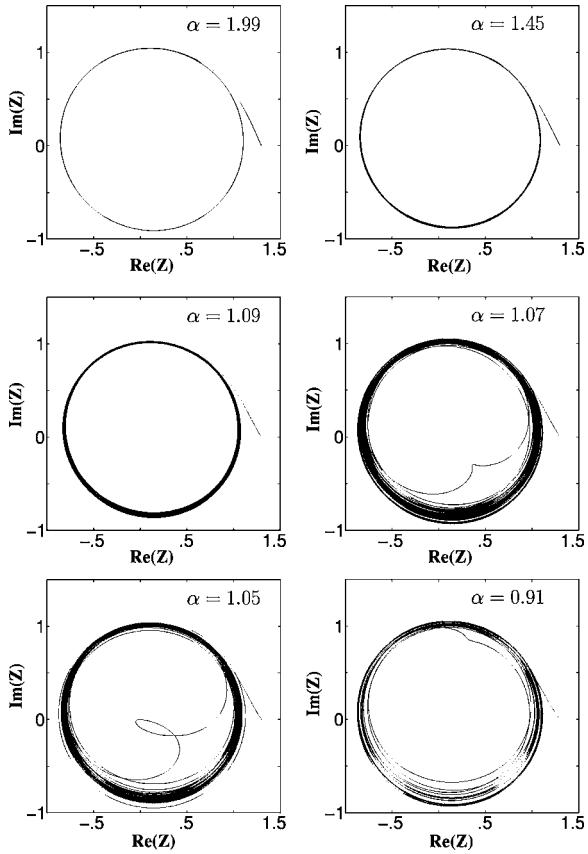


FIG. 6. Broadening of limit cycle. Plane $(\mathrm{Re}\,Z, \mathrm{Im}\,Z)$ shows projection of the complex amplitude $Z=Z(0,t)$ of the central oscillator as a function of time for $\alpha=1.99$, $\alpha=1.45$, $\alpha=1.09$, $\alpha=1.07$, $\alpha=1.05$, $\alpha=0.91$.

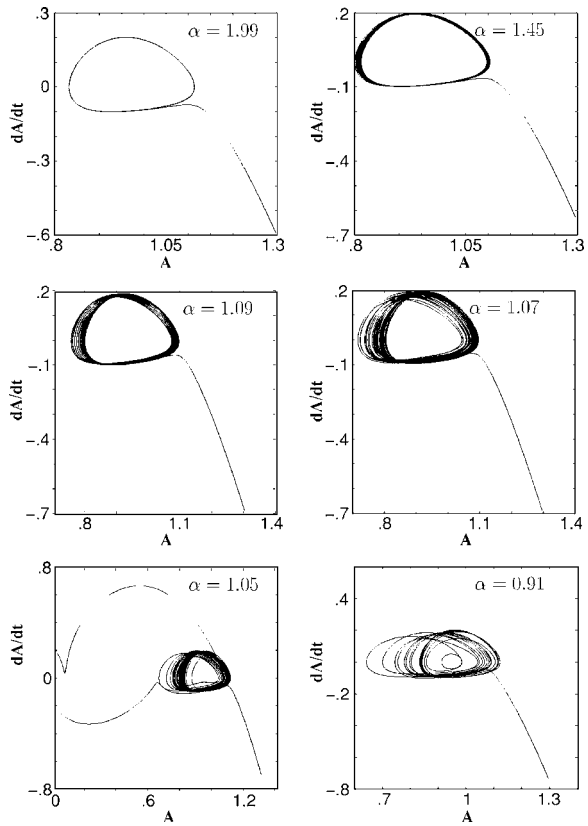


FIG. 7. Broadening of limit cycle. Appearance of topological defect. Plane $(A, dA/dt)$ shows projection of the trajectory of the central oscillator in phase space, where $A(t)=|Z(0,t)|^2$ for $\alpha=1.99$, $\alpha=1.45$, $\alpha=1.09$, $\alpha=1.07$, $\alpha=1.05$, $\alpha=0.91$.

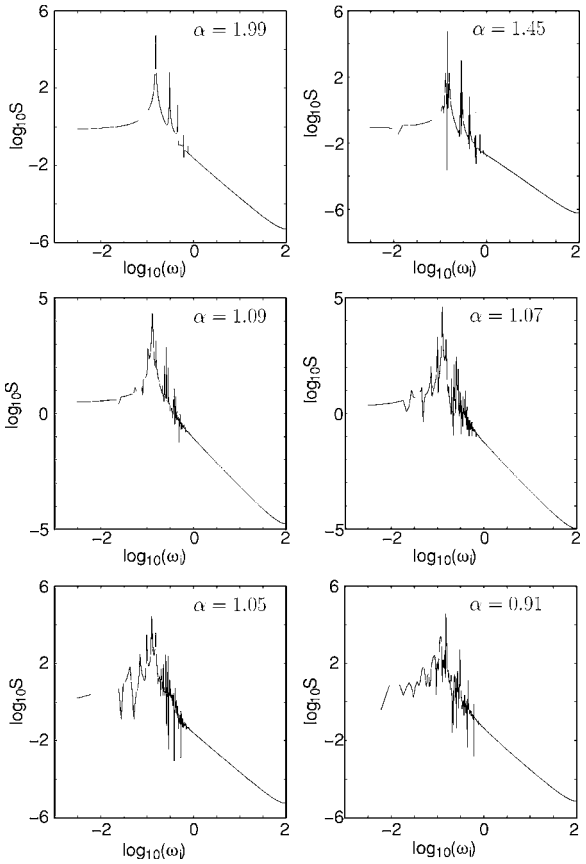


FIG. 8. Broadening of limit cycle. Spectrum of time oscillations of $Z(0,t)$ [see definition in Eq. (35)] for $\alpha=1.99$, $\alpha=1.45$, $\alpha=1.09$, $\alpha=1.07$, $\alpha=1.05$, $\alpha=0.91$.

$$n=\frac{1}{2\pi}\oint_L \nabla\,\theta dl, \tag{45}$$

where $L$ is a contour encircling a zero of $Z$.

For $1<\alpha<2$, we have the limit cycles around the point $A=1$, $dA/dt=0$. It is easy to see the broadening of these limit cycles, when $\alpha$ decreases.

Finally for this section, let us comment on the spectrum of time oscillations of $Z(0,t)$ for different $\alpha$, presented in Fig. 8. The broadening of limit cycle leads to widening of the spectrum. The spectrum is filled out by different harmonics that are localized in the region $0.1<\omega<1$. For $\omega>1$, we have the dependence $S(\omega)\sim\omega^{-2}$ that follows directly from Eq. (12).

## IX. AMPLITUDE DEPENDENCE OF THE TRANSITION TO TURBULENCE

In this section, we would like to show that the turbulent regime developing depends on the initial amplitude. For simulation, we use some parameters as in Eqs. (39) and (26) except for $\alpha=1.45$.

It is seen from Fig. 9, that the decrease of the initial amplitude $A_0$ from 1.3 to 0.005 does not change, at least visually, the space-time structure of turbulence, but the change increases the time of developing an instability and

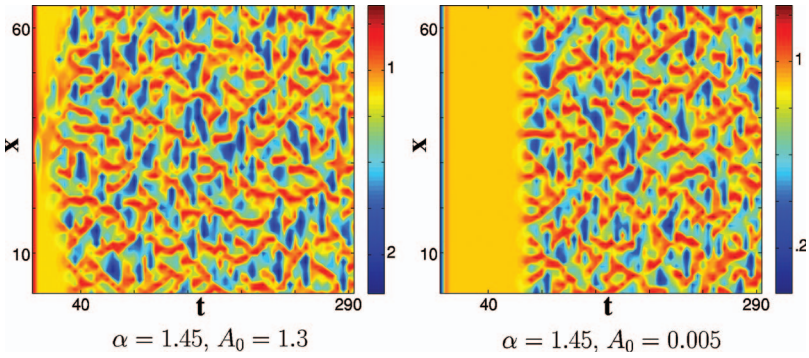


FIG. 9. (Color) Amplitude dependence of transition to turbulence. The decrease of the initial amplitude from 1.3 to 0.005 gives the space-time structure of turbulence almost no change. There is only an increase of time at the beginning of the turbulence.

beginning of turbulence. The turbulence possesses a robustness with respect to change of the amplitude of initial excitation and initial conditions.

In Fig. 10 the plane $(A, dA/dt)$ shows projection of a trajectory of the central oscillator. There are random rotations on the plane and a broadening of the spectrum in a finite region of frequencies. Figure 10 shows many loops of the trajectory for which $dA/dt=0$ and $A$ is close to zero. That means that the turbulent regime includes many different points that are close to the topological defects.

## X. CONCLUSION

The main goal of this paper was to study the influence of long-range interaction (LRI) on the developing of chaotic or turbulent motion in a one-dimensional chain of a large number of nonlinear oscillators. The LRI is characterized by the power of interaction $\alpha$. In the continuous limit the corresponding equation is the nonstationary generalized Ginzburg-Landau (FGL) equation with complex coefficients and fractional derivatives of order $\alpha$ along the coordinate variables. Our preliminary research show different interesting regimes of behavior of the chain depending on the value of $\alpha$. We have observed a synchronized motion of the chain with different complexes, such as defects, chaos, space-time turbulence, traveling waves. The possibility of using a continuous analog of the chain equations such as the FGL equation, simplifies some estimates although it is well-known that discrete model is "more chaotic" than the continuous one.[32] As it was mentioned before, LRI introduced in Refs. 8–10 was aimed to describe some complex media such as mixture of active chemical, biochemical, or magnetic components. Some indirect indication of the presence of LRI follows from the data observation (see, for example, Ref. 33, and references therein). Nevertheless, direct measurement of the LRI in different extended nonlinear systems is still waiting for its revealing.

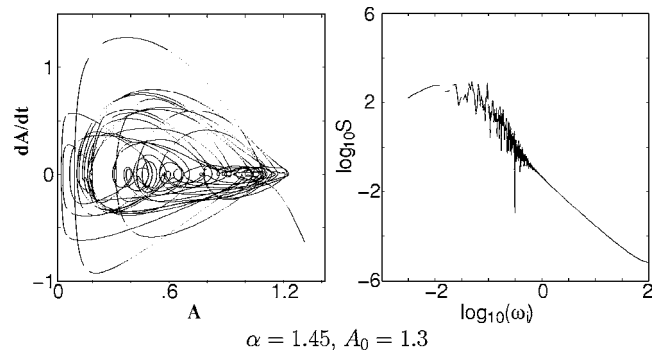


FIG. 10. Amplitude dependence of transition to turbulence. Plane $(A, dA/dt)$ shows projection of the trajectory of the central oscillator in phase space, where $A(t)=|Z(0,t)|^2$, and the spectrum of time oscillations of $Z(0,t)$ for $\alpha=1.45$ and $A=1.3$.

## ACKNOWLEDGMENTS

We are grateful to M. Shlesinger for interesting discussions. This work was supported by the Office of Naval Research, Grant No. N00014-02-1-0056, and the NSF Grant No. DMS-0417800.

[1] M. C. Cross and P. C. Hohenberg, Rev. Mod. Phys. **65**, 851 (1993).
[2] L. M. Pismen, *Vortices in Nonlinear Fields* (Oxford Science, Oxford, 1999).
[3] I. S. Aranson and L. Kramer, Rev. Mod. Phys. **74**, 99 (2002).
[4] D. Tanaka and Y. Kuramoto, Phys. Rev. E **68**, 026219 (2003).
[5] V. Casagrande and A. S. Mikhailov, Physica D **205**, 154 (2005).
[6] S. Shima and Y. Kuramoto, Phys. Rev. E **69**, 036213 (2004).
[7] Y. Kuramoto and D. Battogtokh, Nonlinear Phenom. Complex Syst. (Dordrecht, Neth.) **5**, 380 (2002).
[8] Y. Kuramoto, *Chemical Oscillations, Waves, and Turbulence* (Springer, Berlin, 1984).
[9] A. T. Winfree, J. Theor. Biol. **16**, 15 (1967).
[10] F. J. Dyson, Commun. Math. Phys. **12**, 91 (1969); **12**, 212 (1969); **21**, 269 (1971).
[11] M. Antoni and S. Ruffo, Phys. Rev. E **52**, 2361 (1995).
[12] C. J. Tessone, M. Cencini, and A. Torcini, Phys. Rev. Lett. **97**, 224101 (2006).
[13] V. L. Pokrovsky and A. Virosztek, J. Phys. C **16**, 4513 (1983).
[14] C. Anteneodo and C. Tsallis, Phys. Rev. Lett. **80**, 5313 (1998).
[15] A. Pikovsky, M. Rosenblum, and J. Kurths, *Synchronization. A Universal Concept in Nonlinear Sciences* (Cambridge University Press, Cambridge, 2001).
[16] S. Boccaletti, J. Kurths, G. Osipov, D. L. Valladares, and C. S. Zhou, Phys. Rep. **366**, 1 (2002).
[17] V. E. Tarasov and G. M. Zaslavsky, Chaos **16**, 023110 (2006).
[18] N. Korabel and G. M. Zaslavsky, Physica A **378**, 223 (2007).
[19] H. Weitzner and G. M. Zaslavsky, Commun. Nonlinear Sci. Numer. Simul. **8**, 273 (2003).
[20] A. J. Majda, D. W. McLaughlin, and E. G. Tabak, J. Nonlinear Sci. **7**, 9 (1997).
[21] S. Flach, Phys. Rev. E **58**, R4116 (1998); A. V. Gorbach and S. Flach, *ibid.* **72**, 056607 (2005).
[22] O. M. Braun and Y. S. Kivshar, Phys. Rep. **306**, 2 (1998).
[23] N. Laskin and G. M. Zaslavsky, Physica A **368**, 38 (2006).
[24] V. E. Tarasov and G. M. Zaslavsky, Physica A **383**, 291 (2007).
[25] A. A. Kilbas, H. M. Srivastava, and J. J. Trujillo, *Theory and Application of Fractional Differential Equations* (Elsevier, Amsterdam, 2006).
[26] H. Chate, A. Pikovsky, and O. Rudzick, Physica D **131**, 17 (1999).
[27] H. Chaté, Nonlinearity **7**, 185 (1994).
[28] M. van Hecke, Phys. Rev. Lett. **80**, 1896 (1998).

[29]A. S. Pikovsky, M. G. Rosenblum, and J. Kurths, Int. J. Bifurcation Chaos Appl. Sci. Eng. **10**, 2291 (2000).
[30]G. Friesecke, Physica D **171**, 211 (2002).
[31]D. Treschev, Discrete Contin. Dyn. Syst. **11**, 867 (2004).
[32]G. M. Zaslavsky, *Hamiltonian Chaos and Fractional Dynamics* (Oxford University Press, Oxford, 2005).
[33]Y. Roichman, D. G. Grier, and G. M. Zaslavsky, Phys. Rev. E **75**, 020401 (2007).